

Article

Analytical Solution and Quasi-Periodic Behavior of a Charged Dilaton Black Hole

Ruifang Wang  and Fabao Gao * 

School of Mathematical Science, Yangzhou University, Yangzhou 225002, China; wangruifang16@sina.com

* Correspondence: fbgao@yzu.edu.cn

Abstract: With the vast breakthrough brought by the Event Horizon Telescope, the theoretical analysis of various black holes has become more critical than ever. In this paper, the second-order asymptotic analytical solution of the charged dilaton black hole flow in the spinodal region is constructed from the perspective of dynamics by using the two-timing scale method. Through a numerical comparison with the original charged dilaton black hole system, it is found that the constructed analytical solution is highly consistent with the numerical solution. In addition, several quasi-periodic motions of the charged dilaton black hole flow are numerically obtained under different groups of irrational frequency ratios, and the phase portraits of the black hole flow with sufficiently small thermal parameter perturbation display good stability. Finally, the final evolution state of black hole flow over time is studied according to the obtained analytical solution. The results show that the smaller the integral constant of the system, the greater the periodicity of the black hole flow.

Keywords: charged dilaton black hole; analytical solution; quasi-periodic behavior; extended phase space; two-timing scale method



Citation: Wang, R.; Gao, F. Analytical Solution and Quasi-Periodic Behavior of a Charged Dilaton Black Hole. *Universe* **2021**, *7*, 377. <https://doi.org/10.3390/universe7100377>

Academic Editors: Sergei B. Popov and Ziri Younsi

Received: 2 September 2021

Accepted: 4 October 2021

Published: 9 October 2021

Publisher's Note: MDPI stays neutral with regard to jurisdictional claims in published maps and institutional affiliations.



Copyright: © 2021 by the authors. Licensee MDPI, Basel, Switzerland. This article is an open access article distributed under the terms and conditions of the Creative Commons Attribution (CC BY) license (<https://creativecommons.org/licenses/by/4.0/>).

1. Introduction

The black hole is a spacetime region where the gravity is so strong that any particle (including photons) close to it can be dragged to its center. The earliest paper can be traced back to the pioneering work of Oppenheimer and Snyder [1] in 1939. Visual observation of a real black hole is highly challenging, because it does not reflect light and is too far away from us. Therefore, plenty of researchers have investigated invisible companion stars, namely black holes, based on the visible companion stars of binary systems [2–4]. Nowadays, the research on black holes has involved gravitational waves, wormholes, modified gravitational theory, quantum regime, and several other related fields [5–14].

Black holes can emit thermal radiation. Researchers found a significant analogy between the mathematical form of their physical laws and the laws of thermodynamics as early as the 1970s [15,16], and then the thermodynamic properties of black holes received a lot of attention [17–22]. The similarity between their thermodynamic phase structure and van der Waals fluid system was further proven [23,24]. Moreover, there are a great number of studies on the phase transition of black holes [25–46]. The critical behaviors of different black holes were discussed by depicting the P - V diagrams [25–33]. From these diagrams, one can identify the occurrence of the phase transition and the spinodal region, where the small-black-hole (SBH) and large-black-hole (LBH) coexist. Furthermore, the related homoclinic orbits in the extended phase space were also analyzed. Zhao et al. [34] mainly studied the phase transition process and demonstrated the SBH-LBH-phase coexistence curves' boundary with different parameters in the charged topological dilaton AdS black hole. For the black holes in a higher dimension, such as Gauss-Bonnet-Born-Infeld AdS black holes, some interpretations on their critical behavior can be found in Refs. [35,44]. Dozens of researchers have studied the related critical behavior for the black hole in the extended phase space, where there are prosperous phase structures [11,27,35,43]. Further-

more, from the perspective of phase transition, some properties of the microstructure of the charged AdS black hole can be found in [46].

In order to identify the chaos motions of the Kerr-AdS black hole, Born-Infeld-AdS black hole, charged AdS and dilaton black hole, and charged Gauss-Bonnet AdS black hole, Chen et al. used the Melnikov method to study the temporal and spatial chaos of these black holes [47–51]. They found a critical value δ_c of the perturbation amplitude, which depends on other parameters in the black hole system; the temporal chaos exists in the case $\delta > \delta_c$, while the spatial chaos exists whatever the value of δ is. For the Schwarzschild black hole under the minimal length effects, the same method was also applied to investigate its chaotic behavior [52]. Moreover, there are several references on the chaos motion of the particles around the black holes, including the analyses of the dynamic behavior of the particles, Poincaré surface of section, and innermost stable circular orbits [53–55].

Inspired by the similarity of thermal phase structure and van der Waals fluid system and the literature of different black hole solutions, this paper will mainly use the two-timing scale method (see [56] for more details) and analysis techniques to study the dynamic behavior of a charged dilaton black hole and construct the corresponding analytical solutions from the perspective of dynamics. The two-timing scale method is one of the most effective methods in the quantitative analysis of nonlinear dynamics. It can describe periodic motion and disclose the attenuated vibration of the dissipative system. From the references mentioned earlier, there exist non-chaotic regions under certain conditions. Therefore, considering the temporal thermal perturbation, the quasi-periodic behavior of the charged dilaton black hole flow in the spinodal region will also be discussed and analyzed in the following sections. The layout of this paper is as follows. In Section 2, the equation model of the charged dilaton black hole will be introduced in the extended phase space. In Section 3, the two-timing scale method will be used to solve the dynamic equation of the black hole flow, and the numerical comparison will be carried out in Section 4, where there is a quasi-periodic motion. Accordingly, several kinds of quasi-periodic motion will be shown in Section 5, and the paper ends with the discussion and conclusion.

2. Thermodynamics and Dynamics in the Extended Phase Space

2.1. Equation of State

This section reviews the thermodynamic definition of a charged dilaton black hole solution in the extended phase space. The action of Einstein-Maxwell-dilaton gravity in a four-dimensional spacetime is given by [25,37,48,57,58]

$$I = \frac{1}{16\pi} \int d^4x \sqrt{-g} \left[R - 2(\nabla\phi)^2 - 2\Lambda e^{2\alpha\phi} - \frac{2\alpha^2}{b^2(\alpha^2 - 1)} e^{2\phi/\alpha} - e^{-2\alpha\phi} F_{\mu\nu} F^{\mu\nu} \right], \quad (1)$$

where R is the Ricci scalar, ϕ is the scalar field of dilaton, Λ is the cosmological constant, $F_{\mu\nu}$ is the electromagnetic tensor related to vector potential A_ν . The coupling parameter between the Maxwell and dilaton fields is defined by α , and b is an arbitrary positive constant.

Following the action (1), the metric element describing the spherical symmetric black hole solution can be obtained, i.e., [48,57]

$$ds^2 = -f(r)dt^2 + \frac{1}{f(r)}dr^2 + r^2R(r)^2(d\theta^2 + \sin^2\theta d\phi^2), \quad (2)$$

with

$$f(r) = -\frac{\alpha^2 + 1}{\alpha^2 - 1} \left(\frac{b}{r}\right)^{-2\gamma} - \frac{m}{r^{1-2\gamma}} - \frac{3(\alpha^2 + 1)^2 r^2}{l^2(\alpha^2 - 3)} \left(\frac{b}{r}\right)^{2\gamma} + \frac{q^2(\alpha^2 + 1)}{r^2} \left(\frac{b}{r}\right)^{-2\gamma},$$

$$\phi(r) = \frac{\alpha}{\alpha^2 + 1} \ln\left(\frac{b}{r}\right), \quad R(r) = \left(\frac{b}{r}\right)^\gamma,$$

where q is the charge of the black hole, m is related to the ADM mass M of (2) via $m = 2(\alpha^2 + 1)b^{-2\gamma}M$, and $\gamma = \alpha^2 / (\alpha^2 + 1)$. Note that when $\alpha = 0$, the metric (2) simplifies to the R-N AdS black hole.

In the extended thermodynamic phase space, the thermodynamic pressure P and the volume V , which is the conjugate quantity of P , take the form

$$P = -\frac{(3 + \alpha^2)b^{2\gamma}\Lambda}{8\pi(3 - \alpha^2)r_+^{2\gamma}}, \tag{3}$$

$$V = \frac{4\pi(1 + \alpha^2)b^{2\gamma}}{3 + \alpha^2}r_+^{\frac{3+\alpha^2}{1+\alpha^2}}, \tag{4}$$

where r_+ represents the largest root of $f(r) = 0$, which is the event horizon radius of the black hole. Concerning the first law of thermodynamics, P and V can be written as

$$P = -\frac{\Lambda}{8\pi}, \quad V = \frac{4\pi r_+^3}{3}. \tag{5}$$

Identifying the specific volume v with the event horizon radius of the charged dilaton black hole with

$$v = \frac{2(1 + \alpha^2)(3 - \alpha^2)}{(3 + \alpha^2)}r_+, \tag{6}$$

then the equation of state $P(v, T)$ becomes

$$P(v, T) = \frac{T}{v} + \frac{b^{-2\gamma}}{2^{2\gamma}\pi v^{2(1-\gamma)}(\alpha^2 + 1)^{2(\gamma-2)}} \times \left[\frac{(3 - \alpha^2)^{1-2\gamma}}{2(\alpha^2 - 1)(\alpha^2 + 1)^2(3 + \alpha^2)^{1-2\gamma}} + \frac{2q^2(3 + \alpha^2)^{2\gamma-3}}{v^2(3 - \alpha^2)^{2\gamma-3}} \right]. \tag{7}$$

It describes the relationship between the three thermodynamic parameters (namely pressure P , specific volume v and Hawking temperature T) when the matter is in thermodynamic equilibrium. Note that there is a critical temperature

$$T_{crit} = (\alpha^2 + 1) \left(3 + \alpha^2\right)^{\frac{2\gamma-3}{2}} / \left[\pi b^{2\gamma} q^{1-2\gamma} (1 - \alpha^2)(\alpha^2 + 2)^{\frac{1-2\gamma}{2}}\right],$$

where the second-order phase transition happens (see Refs. [25,48] for more details). For $T_0 < T_{crit}$, $P(v, T)$ have the characteristics:

- (i) $P_v(v, T) < 0$ when $v \in (0, v_\alpha) \cup (v_\beta, \infty)$;
- (ii) $P_v(v, T) > 0$ when $v \in (v_\alpha, v_\beta)$;
- (iii) $P_v(v_\alpha, T_0) = P_v(v_\beta, T_0) = 0$.

2.2. Equation of Dynamics

Combined with the equation of state of the charged dilaton black hole, the thermodynamic equation of the black hole flow is considered in the spinodal region, which is affected by the temporal-periodic perturbation. Thus, the absolute temperature T with a weak time-periodic fluctuation is written as

$$T = T_0 + \epsilon \delta \cos(\omega t) \cos M, \tag{8}$$

where $\epsilon(0 < \epsilon \ll 1)$ is a thermal perturbation parameter, δ is the perturbation amplitude relative to the small viscosity, ω is frequency of the absolute temperature, and T_0 value will be smaller than T_{crit} value.

According to [48–50], there is a charged dilaton black hole flow, which is thermoelastic, slightly viscous, and isotropic, passes along the Eulerian coordinate x -axis in a tube with a fixed volume and unit cross-section. Moreover, the position x of the black hole is a function of the time t and the mass M of the column of fluid of unit cross-section between a fluid particle and the reference fluid particle. Thus, $v(M, t) = \partial x(M, t) / \partial M$ and $u(M, t) = \partial x(M, t) / \partial t$ are the specific volume and the velocity, respectively. Then, x satisfies the following equation

$$\frac{\partial^2 x}{\partial t^2} = -\frac{\partial P(v, T)}{\partial M} + \epsilon \mu_0 s \frac{\partial^2 u}{\partial M^2} - A s^2 \frac{\partial^3 v}{\partial M^3}, \tag{9}$$

where the expression of $P(v, T)$ is shown as (10), μ_0 is a positive parameter related to the viscosity, s is a positive parameter, and A is a positive constant (see Ref. [48] for more details).

$$\begin{aligned} P(v, T) = & P(v_0, T_0) + P_v(v_0, T_0)(v - v_0) + P_T(v_0, T_0)(T - T_0) \\ & + P_{vT}(v_0, T_0)(v - v_0)(T - T_0) + \frac{P_{vvv}(v_0, T_0)}{3!}(v - v_0)^3 \\ & + \frac{P_{vvT}(v_0, T_0)}{2}(v - v_0)^2(T - T_0) + \dots, \end{aligned} \tag{10}$$

with

$$\begin{aligned} P_T(v_0, T_0) &= \frac{1}{v_0}, \quad P_{vT}(v_0, T_0) = -\frac{1}{v_0^2}, \quad P_{vvv}(v_0, T_0) = \frac{2}{v_0^3}, \\ P_v(v_0, T_0) &= -\frac{T_0}{v_0^2} + \frac{[(3 - \alpha^2)(\alpha^2 + 1)]^{\frac{1-\alpha^2}{\alpha^2+1}}}{\pi(1 - \alpha^2)4^{\frac{\alpha^2}{\alpha^2+1}}b^{\frac{2\alpha^2}{\alpha^2+1}}(\alpha^2 + 3)^{\frac{\alpha^2+3}{\alpha^2+1}}v_0^{\frac{3\alpha^2+5}{\alpha^2+1}}} \\ &\quad \times \left[4(\alpha^4 + \alpha^2 - 2)(\alpha^4 - 2\alpha^2 - 3)^2 q^2 + (\alpha^2 + 3)^2 v_0^2 \right], \\ P_{vvv}(v_0, T_0) &= -\frac{6T_0}{v_0^4} + \frac{2(3 - \alpha^2)^{\frac{1-\alpha^2}{1+\alpha^2}}(\alpha^2 + 2)}{\pi(1 - \alpha^2)4^{\frac{\alpha^2}{\alpha^2+1}}b^{\frac{2\alpha^2}{\alpha^2+1}}(\alpha^2 + 1)^{\frac{3\alpha^2+1}{\alpha^2+1}}(\alpha^2 + 3)^{\frac{\alpha^2+3}{\alpha^2+1}}v_0^{\frac{5\alpha^2+7}{\alpha^2+1}}} \\ &\quad \times \left[(\alpha^2 + 3)^3 v_0^2 + 4(\alpha^2 - 1)(2\alpha^2 + 3)(3\alpha^2 + 5)(\alpha^4 - 2\alpha^2 - 3)^2 q^2 \right]. \end{aligned}$$

where v_0 is the inflection point in the spinodal region, which satisfies $\partial^2 P / \partial^2 v = 0$ at v_0 .

Expand the functions $v(M, t)$ and $u(M, t)$ in Fourier series with respect to $M \in [0, 2\pi]$ near v_0 as

$$v(M, t) = v_0 + x_1(t) \cos M + x_2(t) \cos 2M + x_3(t) \cos 3M + \dots, \tag{11}$$

$$u(x, t) = u_1(t) \sin M + u_2(t) \sin 2M + u_3(t) \sin 3M + \dots, \tag{12}$$

where $x_i(t)$ and $u_i(t)$ are regarded as the position and velocity of the hydrodynamical modes, respectively (see [49,50,59,60] for details). Consider the first two modes, i.e., $x_n(t) = u_n(t) = 0$ when $n \geq 3$, the Equation (9) become (omit (v_0, T_0))

$$\begin{aligned}
 \dot{x}_1 &= u_1, \\
 \dot{x}_2 &= u_2, \\
 \dot{u}_1 &= \left(P_v - As^2 \right) x_1 + \epsilon \left(P_T + \frac{P_{vT}}{2} x_2 + \frac{3P_{vvT}}{8} x_1^2 + \frac{P_{vvT}}{4} x_2^2 \right) \delta \cos \omega t \\
 &\quad + \frac{P_{vvv}}{8} \left(x_1^3 + 2x_1 x_2^2 \right) - \epsilon \mu_0 s u_1, \\
 \dot{u}_2 &= \left(P_v - 4As^2 \right) x_2 + \epsilon \left(\frac{P_{vT}}{2} x_1 + \frac{P_{vvT}}{2} x_1 x_2 \right) \delta \cos \omega t \\
 &\quad + \frac{P_{vvv}}{8} \left(x_2^3 + 2x_1^2 x_2 \right) - 4\epsilon \mu_0 s u_2.
 \end{aligned}
 \tag{13}$$

Now we transform the dynamical equations of the charged dilaton black hole (13) into the form of second-order differential equations

$$\begin{aligned}
 \ddot{x}_1 + \epsilon \mu_0 s \dot{x}_1 + \left(As^2 - P_v \right) x_1 - \frac{P_{vvv}}{8} x_1^3 - \frac{P_{vvv}}{4} x_1 x_2^2 \\
 = \epsilon \left(P_T + \frac{P_{vT}}{2} x_2 + \frac{3P_{vvT}}{8} x_1^2 + \frac{P_{vvT}}{4} x_2^2 \right) \delta \cos \omega t, \\
 \ddot{x}_2 + 4\epsilon \mu_0 s \dot{x}_2 + \left(4As^2 - P_v \right) x_2 - \frac{P_{vvv}}{8} x_2^3 - \frac{P_{vvv}}{4} x_1^2 x_2 \\
 = \epsilon \left(P_{vT} x_1 + \frac{P_{vvT}}{2} x_1 x_2 \right) \delta \cos \omega t.
 \end{aligned}
 \tag{14}$$

3. Two-Timing Scale Method Solution

In this section, the asymptotic analytical solutions of the charged dilaton black hole are studied by using the two-timing scale method [56]. Suppose that the approximate solutions of the system (14) take the form

$$\begin{aligned}
 x_1(t, \epsilon) &= \epsilon x_{11}(T_1, T_2) + \epsilon^2 x_{12}(T_1, T_2), \\
 x_2(t, \epsilon) &= \epsilon x_{21}(T_1, T_2) + \epsilon^2 x_{22}(T_1, T_2),
 \end{aligned}
 \tag{15}$$

where the two-timing scales are defined as $T_1 = t$ and $T_2 = \epsilon t$, respectively.

Denote

$$\begin{aligned}
 \dot{x}_{ij} &= \frac{\partial x_{ij}}{\partial T_1} \frac{\partial T_1}{\partial t} + \frac{\partial x_{ij}}{\partial T_2} \frac{\partial T_2}{\partial t} \\
 &= \frac{\partial x_{ij}}{\partial T_1} + \epsilon \frac{\partial x_{ij}}{\partial T_2} \\
 &\triangleq \partial_{T_1} x_{ij} + \epsilon \partial_{T_2} x_{ij},
 \end{aligned}
 \tag{16}$$

$$\begin{aligned}
 \ddot{x}_{ij} &= \frac{\partial}{\partial t} \left(\frac{\partial x_{ij}}{\partial T_1} + \epsilon \frac{\partial x_{ij}}{\partial T_2} \right) \\
 &= \frac{\partial^2 x_{ij}}{\partial T_1^2} \frac{\partial T_1}{\partial t} + \frac{\partial^2 x_{ij}}{\partial T_1 T_2} \frac{\partial T_2}{\partial t} + \epsilon \frac{\partial^2 x_{ij}}{\partial T_2 T_1} \frac{\partial T_1}{\partial t} + \epsilon \frac{\partial^2 x_{ij}}{\partial T_2^2} \frac{\partial T_2}{\partial t} \\
 &\triangleq \partial_{T_1 T_1} x_{ij} + 2\epsilon \partial_{T_1 T_2} x_{ij} + \epsilon^2 \partial_{T_2 T_2} x_{ij},
 \end{aligned}
 \tag{17}$$

where $i, j = 1, 2$. Then, substituting Equations (15)–(17) into Equation (14) and comparing the coefficients of powers of ϵ , one obtains

$$\begin{aligned}
 \epsilon^1 : \partial_{T_1 T_1} x_{11} + \left(As^2 - P_v \right) x_{11} - P_T \delta \cos \omega T_1 &= 0, \\
 \partial_{T_1 T_1} x_{21} + \left(4As^2 - P_v \right) x_{21} &= 0, \\
 \epsilon^2 : \partial_{T_1 T_1} x_{12} + \left(As^2 - P_v \right) x_{12} + 2\partial_{T_1 T_2} x_{11} + \mu_0 s \partial_{T_1} x_{11} - \frac{P_{vT}}{2} x_{21} \delta \cos \omega T_1 &= 0,
 \end{aligned}
 \tag{18}$$

$$\partial_{T_1 T_1} x_{22} + (4As^2 - P_v) x_{22} + 2\partial_{T_1 T_2} x_{21} + 4\mu_0 s \partial_{T_1} x_{21} - P_{vT} x_{11} \delta \cos \omega T_1 = 0, \tag{19}$$

$$\begin{aligned} \epsilon^3 : \partial_{T_1 T_1} x_{13} + (As^2 - P_v) x_{13} + \partial_{T_2 T_2} x_{11} + 2\partial_{T_1 T_2} x_{12} + \mu_0 s (\partial_{T_2} x_{11} + \partial_{T_1} x_{12}) \\ - \left(\frac{P_{vT}}{2} x_{22} + \frac{3P_{vvT}}{8} x_{11}^2 + \frac{P_{vvT}}{4} x_{21}^2 \right) \delta \cos \omega T_1 - \frac{P_{vvv}}{8} x_{11}^3 - \frac{P_{vvv}}{4} x_{11} x_{21}^2 = 0, \\ \partial_{T_1 T_1} x_{23} + (4As^2 - P_v) x_{23} + \partial_{T_2 T_2} x_{21} + 2\partial_{T_1 T_2} x_{22} + 4\mu_0 s (\partial_{T_2} x_{21} + \partial_{T_1} x_{22}) \\ - \left(P_{vT} x_{12} + \frac{P_{vvT}}{2} x_{11} x_{21} \right) \delta \cos \omega T_1 - \frac{P_{vvv}}{8} x_{21}^3 - \frac{P_{vvv}}{4} x_{11}^2 x_{21} = 0. \end{aligned} \tag{20}$$

Note that the works of temporal and spatial chaos of system (14) had been done in Ref. [59] when $\frac{P_v}{4A} < s^2 < \frac{P_v}{A}$. We now consider the case $s^2 \geq \frac{P_v}{A}$, i.e., $As^2 - P_v \geq 0$, and take the case of non-resonance into consideration, i.e., $\omega^2 \neq \lambda_i^2 (i = 1, 2)$ and $|\lambda_1 \pm \lambda_2| \neq \omega$.

Let $\lambda_1 = \sqrt{As^2 - P_v}$, $\lambda_2 = \sqrt{4As^2 - P_v}$. Then, Equation (18) have the general solutions

$$\begin{aligned} x_{11}(T_1, T_2) = G_1(T_2)e^{i\lambda_1 T_1} + \overline{G_1(T_2)}e^{-i\lambda_1 T_1} - \frac{P_T \delta}{2(\omega^2 - \lambda_1^2)} \left(e^{i\omega T_1} + e^{-i\omega T_1} \right), \\ x_{21}(T_1, T_2) = G_2(T_2)e^{i\lambda_2 T_1} + \overline{G_2(T_2)}e^{-i\lambda_2 T_1}, \end{aligned} \tag{21}$$

where $G_i (i = 1, 2)$ is a function of the time-scale T_2 and $\overline{G_i}$ denotes the conjugate quantity of G_i . Substituting Equation (21) into Equation (19), yields

$$\begin{aligned} \partial_{T_1 T_1} x_{12} + \lambda_1^2 x_{12} = -2i\lambda_1 e^{i\lambda_1 T_1} \partial_{T_2} G_1 + 2i\lambda_1 e^{-i\lambda_1 T_1} \partial_{T_2} \overline{G_1} - \mu_0 s \left[i\lambda_1 G_1 e^{i\lambda_1 T_1} \right. \\ \left. - \frac{P_T \delta i \omega}{2(\omega^2 - \lambda_1^2)} e^{i\omega T_1} - i\lambda_1 \overline{G_1} e^{-i\lambda_1 T_1} - \frac{P_T \delta i \omega}{2(\omega^2 - \lambda_1^2)} e^{-i\omega T_1} \right] \\ + \frac{P_{vT} \delta}{4} \left[G_2 e^{i(\lambda_2 + \omega) T_1} + G_2 e^{i(\lambda_2 - \omega) T_1} + \overline{G_2} e^{i(\omega - \lambda_2) T_1} \right. \\ \left. + \overline{G_2} e^{-i(\lambda_2 + \omega) T_1} \right], \\ \partial_{T_1 T_1} x_{22} + \lambda_2^2 x_{22} = -2i\lambda_2 e^{i\lambda_2 T_1} \partial_{T_2} G_2 + 2i\lambda_2 e^{-i\lambda_2 T_1} \partial_{T_2} \overline{G_2} - 4\mu_0 s \left(i\lambda_2 e^{i\lambda_2 T_1} G_2 \right. \\ \left. - i\lambda_2 e^{-i\lambda_2 T_1} \overline{G_2} \right) + \frac{P_{vT} \delta}{2} \left[G_1 e^{i(\lambda_1 + \omega) T_1} + G_1 e^{i(\lambda_1 - \omega) T_1} \right. \\ \left. - \frac{P_T \delta}{2(\omega^2 - \lambda_1^2)} e^{2i\omega T_1} - \frac{P_T \delta}{2(\omega^2 - \lambda_1^2)} + \overline{G_1} e^{i(-\lambda_1 + \omega) T_1} \right. \\ \left. + \overline{G_1} e^{-i(\lambda_1 + \omega) T_1} - \frac{P_T \delta}{2(\omega^2 - \lambda_1^2)} - \frac{P_T \delta}{2(\omega^2 - \lambda_1^2)} e^{-2i\omega T_1} \right]. \end{aligned} \tag{22}$$

To eliminate the secular terms of the above equations, let

$$\begin{aligned} -2i\lambda_1 \partial_{T_2} G_1 - \mu_0 s i \lambda_1 G_1 = 0, \\ -2i\lambda_2 \partial_{T_2} G_2 - 4\mu_0 s i \lambda_2 G_2 = 0. \end{aligned}$$

Then the coefficients G_1 and G_2 are

$$\begin{aligned} G_1(T_2) = c_1 e^{-\frac{\mu_0 s}{2} T_2}, \\ G_2(T_2) = c_2 e^{-2\mu_0 s T_2}, \end{aligned}$$

where c_1 and c_2 are integration constants. Thus, the special solutions of Equation (18) become

$$\begin{aligned} x_{11}(T_1, T_2) &= 2c_1 e^{-\frac{\mu_0 s}{2} T_2} \cos \lambda_1 T_1 - \frac{P_T \delta}{\omega^2 - \lambda_1^2} \cos \omega T_1, \\ x_{22}(T_1, T_2) &= 2c_2 e^{-2\mu_0 s T_2} \cos \lambda_2 T_1. \end{aligned} \tag{23}$$

Therefore, Equation (22) are reduced to

$$\begin{aligned} \partial_{T_1 T_1} x_{12} + \lambda_1^2 x_{12} &= \frac{\mu_0 s P_T \delta i \omega}{2(\omega^2 - \lambda_1^2)} \left(e^{i\omega T_1} - e^{-i\omega T_1} \right) + \frac{c_2 P_{vT} \delta e^{-2\mu_0 s T_2}}{4} \times \\ &\quad \left[e^{i(\lambda_2 + \omega) T_1} + e^{i(\lambda_2 - \omega) T_1} + e^{i(\omega - \lambda_2) T_1} + e^{-i(\lambda_2 + \omega) T_1} \right], \\ \partial_{T_1 T_1} x_{22} + \lambda_2^2 x_{22} &= \frac{c_1 P_{vT} \delta e^{-\frac{\mu_0 s}{2} T_2}}{2} \left[e^{i(\lambda_1 + \omega) T_1} + e^{i(\lambda_1 - \omega) T_1} + e^{i(\omega - \lambda_1) T_1} \right. \\ &\quad \left. + e^{-i(\lambda_1 + \omega) T_1} \right] - \frac{P_{vT} P_T \delta^2}{4(\omega^2 - \lambda_1^2)} \left(e^{2i\omega T_1} + e^{-2i\omega T_1} + 2 \right). \end{aligned} \tag{24}$$

Similarly, suppose that the solutions of Equation (24) are

$$\begin{aligned} x_{12}(T_1, T_2) &= K_1(T_2) e^{i\lambda_1 T_1} + \overline{K_1(T_2)} e^{-i\lambda_1 T_1} - \frac{\mu_0 s P_T \delta i \omega}{2(\lambda_1^2 - \omega^2)^2} \left(e^{i\omega T_1} - e^{-i\omega T_1} \right) \\ &\quad + \frac{c_2 P_T \delta e^{-2\mu_0 s T_2}}{4 \left[\lambda_1^2 - (\lambda_2 + \omega)^2 \right]} \left[e^{i(\lambda_2 + \omega) T_1} + e^{-i(\lambda_2 + \omega) T_1} \right] \\ &\quad + \frac{c_2 P_T \delta e^{-2\mu_0 s T_2}}{4 \left[\lambda_1^2 - (\lambda_2 - \omega)^2 \right]} \left[e^{i(\lambda_2 - \omega) T_1} + e^{i(\omega - \lambda_2) T_1} \right], \\ x_{22}(T_1, T_2) &= K_2(T_2) e^{i\lambda_2 T_1} + \overline{K_2(T_2)} e^{-i\lambda_2 T_1} + \frac{c_1 P_{vT} \delta e^{-\frac{\mu_0 s}{2} T_2}}{4 \left[\lambda_2^2 - (\lambda_1 + \omega)^2 \right]} \left[e^{i(\lambda_1 + \omega) T_1} \right. \\ &\quad \left. + e^{-i(\lambda_1 + \omega) T_1} \right] + \frac{c_1 P_{vT} \delta e^{-\frac{\mu_0 s}{2} T_2}}{4 \left[\lambda_2^2 - (\lambda_1 - \omega)^2 \right]} \left[e^{i(\lambda_1 - \omega) T_1} + e^{i(\omega - \lambda_1) T_1} \right] \\ &\quad - \frac{P_{vT} P_T \delta^2}{4(\omega^2 - \lambda_1^2)(\lambda_2^2 - 4\omega^2)} \left(e^{2i\omega T_1} + e^{-2i\omega T_1} \right) - \frac{P_{vT} P_T \delta^2}{4(\omega^2 - \lambda_1^2)\lambda_2^2}. \end{aligned} \tag{25}$$

Substituting Equations (23) and (25) into Equation (20), it follows

$$\begin{aligned} \partial_{T_1 T_1} x_{13} + \lambda_1^2 x_{13} &= -\frac{c_1 \mu_0^2 s^2 e^{-\frac{\mu_0 s}{2} T_2}}{4} \left(e^{i\lambda_1 T_1} + e^{-i\lambda_1 T_1} \right) - 2i\lambda_1 \partial_{T_2} K_1 e^{i\lambda_1 T_1} \\ &\quad + 2i\lambda_1 \partial_{T_2} \overline{K_1} e^{-i\lambda_1 T_1} + \frac{c_2 P_T \delta \mu_0 s i (\lambda_2 + \omega) e^{-2\mu_0 s T_2}}{\lambda_1^2 - (\lambda_2 + \omega)^2} \left[e^{i(\lambda_2 + \omega) T_1} - e^{-i(\lambda_2 + \omega) T_1} \right] \\ &\quad + \frac{c_2 P_T \delta \mu_0 s i (\lambda_2 - \omega) e^{-2\mu_0 s T_2}}{\lambda_1^2 - (\lambda_2 - \omega)^2} \left[e^{i(\lambda_2 - \omega) T_1} - e^{i(\omega - \lambda_2) T_1} \right] - \mu_0 s \left\{ i\lambda_1 K_1 e^{i\lambda_1 T_1} \right. \\ &\quad \left. - i\lambda_1 \overline{K_1} e^{-i\lambda_1 T_1} - \frac{c_1 \mu_0 s e^{-\frac{\mu_0 s}{2} T_2}}{2} \left(e^{i\lambda_1 T_1} + e^{-i\lambda_1 T_1} \right) + \frac{\mu_0 s P_T \delta \omega^2}{2(\lambda_1^2 - \omega^2)^2} \times \right. \\ &\quad \left. \left(e^{i\omega T_1} + e^{-i\omega T_1} \right) + \frac{c_2 P_T \delta i (\lambda_2 + \omega) e^{-2\mu_0 s T_2}}{4 \left[\lambda_1^2 - (\lambda_2 + \omega)^2 \right]} \left[e^{i(\lambda_2 + \omega) T_1} - e^{-i(\lambda_2 + \omega) T_1} \right] \right\} \end{aligned}$$

$$\begin{aligned}
 & + \frac{c_2 P_T \delta i (\lambda_2 - \omega) e^{-2\mu_0 s T_2}}{4 [\lambda_1^2 - (\lambda_2 - \omega)^2]} \left[e^{i(\lambda_2 - \omega) T_1} - e^{i(\omega - \lambda_2) T_1} \right] \Big\} \\
 & + \frac{P_{vT} \delta}{4} \left(e^{i\omega T_1} + e^{-i\omega T_1} \right) \left\{ K_2 e^{i\lambda_2 T_1} + \bar{K}_2 e^{-i\lambda_2 T_1} - \frac{P_{vT} P_T \delta^2}{4(\omega^2 - \lambda_1^2) \lambda_2^2} \right. \\
 & - \frac{P_{vT} P_T \delta^2}{4(\omega^2 - \lambda_1^2)(\lambda_2^2 - \omega^2)} \left(e^{2i\omega T_1} + e^{-2i\omega T_1} \right) \\
 & + \frac{c_1 P_{vT} \delta e^{-\frac{\mu_0 s}{2} T_2}}{4 [\lambda_2^2 - (\lambda_1 - \omega)^2]} \left[e^{i(\lambda_1 - \omega) T_1} + e^{i(\omega - \lambda_1) T_1} \right] \\
 & + \left. \frac{c_1 P_{vT} \delta e^{-\frac{\mu_0 s}{2} T_2}}{4 [\lambda_2^2 - (\lambda_1 + \omega)^2]} \left[e^{i(\lambda_1 + \omega) T_1} + e^{-i(\lambda_1 + \omega) T_1} \right] \right\} \\
 & + \frac{3 P_{vvT} \delta}{16} \left(e^{i\omega T_1} + e^{-i\omega T_1} \right) \left\{ c_1^2 e^{-\mu_0 s T_2} \left(e^{2i\lambda_1 T_1} + e^{-2i\lambda_1 T_1} + 2 \right) \right. \\
 & - \frac{c_1 P_T \delta e^{-\frac{\mu_0 s}{2} T_2}}{\omega^2 - \lambda_1^2} \left[e^{i(\lambda_1 + \omega) T_1} + e^{i(\lambda_1 - \omega) T_1} + e^{i(\omega - \lambda_1) T_1} + e^{-i(\lambda_1 + \omega) T_1} \right] + \\
 & \left. \frac{P_T^2 \delta^2}{4(\omega^2 - \lambda_1^2)^2} \left(e^{2i\omega T_1} + e^{-2i\omega T_1} + 2 \right) \right\} + \frac{c_2^2 P_{vvT} \delta e^{-4\mu_0 s T_2}}{8} \left(e^{i\omega T_1} + e^{-i\omega T_1} \right) \times \\
 & \left(e^{2i\lambda_2 T_1} + e^{-2i\lambda_2 T_1} + 2 \right) + \frac{P_{vvv}}{8} x_{11}^3 - \frac{P_{vvv}}{4} x_{11} x_{21}^2,
 \end{aligned}$$

$$\begin{aligned}
 \partial_{T_1 T_1} x_{23} + \lambda_2^2 x_{23} & = -4c_2 \mu_0^2 s^2 e^{-2\mu_0 s T_2} \left(e^{i\lambda_2 T_1} + e^{-i\lambda_2 T_1} \right) - 2i\lambda_2 \partial_{T_2} K_2 e^{i\lambda_2 T_1} \\
 & + 2i\lambda_2 \partial_{T_2} \bar{K}_2 e^{-i\lambda_2 T_1} + \frac{c_1 P_{vT} \delta \mu_0 s i (\lambda_1 + \omega) e^{-\frac{\mu_0 s}{2} T_2}}{4 [\lambda_2^2 - (\lambda_1 + \omega)^2]} \left[e^{i(\lambda_1 + \omega) T_1} - e^{-i(\lambda_1 + \omega) T_1} \right] \\
 & + \frac{c_1 P_{vT} \delta \mu_0 s i (\lambda_1 - \omega) e^{-\frac{\mu_0 s}{2} T_2}}{4 [\lambda_2^2 - (\lambda_1 - \omega)^2]} \left[e^{i(\lambda_1 - \omega) T_1} - e^{i(\omega - \lambda_1) T_1} \right] \\
 & - 4\mu_0 s \left\{ i\lambda_2 K_2 e^{i\lambda_2 T_1} - i\lambda_2 \bar{K}_2 e^{-i\lambda_2 T_1} - 2c_2 \mu_0 s e^{-2\mu_0 s T_2} \left(e^{i\lambda_2 T_1} + e^{-i\lambda_2 T_1} \right) \right. \\
 & + \frac{c_1 P_{vT} \delta i (\lambda_1 + \omega) e^{-\frac{\mu_0 s}{2} T_2}}{4 [\lambda_2^2 - (\lambda_1 + \omega)^2]} \left[e^{i(\lambda_1 + \omega) T_1} - e^{-i(\lambda_1 + \omega) T_1} \right] \\
 & + \frac{c_1 P_{vT} \delta i (\lambda_1 - \omega) e^{-\frac{\mu_0 s}{2} T_2}}{4 [\lambda_2^2 - (\lambda_1 - \omega)^2]} \left[e^{i(\lambda_1 - \omega) T_1} - e^{-i(\omega - \lambda_1) T_1} \right] \\
 & - \left. \frac{P_{vT} P_T \delta^2 i \omega}{2(\omega^2 - \lambda_1^2)(\lambda_2^2 - 4\omega^2)} \left(e^{2i\omega T_1} - e^{-2i\omega T_1} \right) \right\} + \frac{P_{vT} \delta}{2} \left(e^{i\omega T_1} + e^{-i\omega T_1} \right) \times \\
 & \left\{ K_1 e^{i\lambda_1 T_1} + \bar{K}_1 e^{-i\lambda_1 T_1} + \frac{c_2 P_T \delta e^{-2\mu_0 s T_2}}{4 [\lambda_1^2 - (\lambda_2 + \omega)^2]} \left[e^{i(\lambda_2 + \omega) T_1} + e^{-i(\lambda_2 + \omega) T_1} \right] \right. \\
 & + \left. \frac{c_2 P_T \delta e^{-2\mu_0 s T_2}}{4 [\lambda_1^2 - (\lambda_2 - \omega)^2]} \left[e^{i(\lambda_2 - \omega) T_1} + e^{i(\omega - \lambda_2) T_1} \right] - \frac{\mu_0 s P_T \delta i \omega}{2(\lambda_1^2 - \omega^2)^2} \left(e^{i\omega T_1} - e^{-i\omega T_1} \right) \right\}
 \end{aligned}$$

$$\begin{aligned}
 & + \frac{c_2 P_{vvT} \delta e^{-2\mu_0 s T_2}}{4} \left(e^{i(\lambda_2 + \omega) T_1} + e^{i(\lambda_2 - \omega) T_1} + e^{i(\omega - \lambda_2) T_1} + e^{-i(\lambda_2 + \omega) T_1} \right) \times \\
 & \left[c_1 e^{-\frac{\mu_0 s}{2} T_2} \left(e^{i\lambda_1 T_1} + e^{-i\lambda_1 T_1} \right) - \frac{P_v \delta}{2(\omega^2 - \lambda_1^2)} \left(e^{i\omega T_1} + e^{-i\omega T_1} \right) \right] \\
 & + \frac{c_2^3 P_{vvv} e^{-6\mu_0 s T_2}}{8} \left(e^{3i\lambda_2 T_1} + 3e^{i\lambda_2 T_1} + 3e^{-i\lambda_2 T_1} + e^{-3i\lambda_2 T_1} \right) + \frac{P_{vvv}}{4} x_{11}^2 x_{21}, \tag{26}
 \end{aligned}$$

where the complex expressions of x_{11}^3 , $x_{11}x_{21}^2$ and $x_{11}^2x_{21}$ are shown in Appendix A. To eliminate the secular terms of the Equation (26), we take

$$\begin{aligned}
 K_1(T_2) &= c_3 e^{-\frac{\mu_0 s}{2} T_2}, \\
 K_2(T_2) &= c_4 e^{-2\mu_0 s T_2},
 \end{aligned}$$

where c_3 and c_4 are integration constants. Thus, it leads to the special solutions of Equation (19) as

$$\begin{aligned}
 x_{12}(T_1, T_2) &= 2c_3 e^{-\frac{\mu_0 s}{2} T_2} \cos \lambda_1 T_1 + \frac{\mu_0 s P_T \delta \omega}{(\lambda_1^2 - \omega^2)^2} \sin \omega T_1 \\
 &+ \frac{c_2 P_T \delta e^{-2\mu_0 s T_2}}{2[\lambda_1^2 - (\lambda_2 + \omega)^2]} \cos(\lambda_2 + \omega) T_1 \\
 &+ \frac{c_2 P_T \delta e^{-2\mu_0 s T_2}}{2[\lambda_1^2 - (\lambda_2 - \omega)^2]} \cos(\lambda_2 - \omega) T_1, \\
 x_{22}(T_1, T_2) &= 2c_4 e^{-2\mu_0 s T_2} \cos \lambda_2 T_1 - \frac{P_{vT} P_T \delta^2}{4(\omega^2 - \lambda_1^2) \lambda_2^2} \\
 &- \frac{P_{vT} P_T \delta^2}{2(\omega^2 - \lambda_1^2)(\lambda_2^2 - 4\omega^2)} \cos 2\omega T_1 \\
 &+ \frac{c_1 P_{vT} \delta e^{-\frac{\mu_0 s}{2} T_2}}{2[\lambda_2^2 - (\lambda_1 + \omega)^2]} \cos(\lambda_1 + \omega) T_1 \\
 &+ \frac{c_1 P_{vT} \delta e^{-\frac{\mu_0 s}{2} T_2}}{2[\lambda_2^2 - (\lambda_1 - \omega)^2]} \cos(\lambda_1 - \omega) T_1. \tag{27}
 \end{aligned}$$

Submitting the Equations (23) and (27) into the Equation (15), the solutions of the original system (14) can be obtained as follows

$$\begin{aligned}
 x_1 &= \epsilon \left(2c_1 e^{-\frac{\mu_0 s}{2} T_2} \cos \lambda_1 T_1 - \frac{P_T \delta}{\omega^2 - \lambda_1^2} \cos \omega T_1 \right) + \epsilon^2 \left\{ 2c_3 e^{-\frac{\mu_0 s}{2} T_2} \cos \lambda_1 T_1 \right. \\
 &+ \frac{\mu_0 s P_T \delta \omega}{(\lambda_1^2 - \omega^2)^2} \sin \omega T_1 + \frac{c_2 P_T \delta e^{-2\mu_0 s T_2}}{2[\lambda_1^2 - (\lambda_2 + \omega)^2]} \cos(\lambda_2 + \omega) T_1 \\
 &\left. + \frac{c_2 P_T \delta e^{-2\mu_0 s T_2}}{2[\lambda_1^2 - (\lambda_2 - \omega)^2]} \cos(\lambda_2 - \omega) T_1 \right\}, \\
 x_2 &= \epsilon \left(2c_2 e^{-2\mu_0 s T_2} \cos \lambda_2 T_1 \right) + \epsilon^2 \left\{ 2c_4 e^{-2\mu_0 s T_2} \cos \lambda_2 T_1 - \frac{P_{vT} P_T \delta^2}{4(\omega^2 - \lambda_1^2) \lambda_2^2} \right. \\
 &\left. + \frac{c_1 P_{vT} \delta e^{-\frac{\mu_0 s}{2} T_2}}{2[\lambda_2^2 - (\lambda_1 + \omega)^2]} \cos(\lambda_1 + \omega) T_1 - \frac{P_{vT} P_T \delta^2}{2(\omega^2 - \lambda_1^2)(\lambda_2^2 - 4\omega^2)} \cos 2\omega T_1 \right\}
 \end{aligned}$$

$$+ \frac{c_1 P_{vT} \delta e^{-\frac{\mu_0 s}{2} T_2}}{2[\lambda_2^2 - (\lambda_1 - \omega)^2]} \cos(\lambda_1 - \omega) T_1 \Big\}. \tag{28}$$

4. Numerical Comparison

In order to verify the validity of the calculation results, a numerical comparison is carried out in this section. Consider the case $T_0 = 0.0315$ and $\epsilon = 0.001$, and consequently $v_0 = 3.652$. The initial value of the charged dilaton black hole system is selected as $[x_1(0), u_1(0), x_2(0), u_2(0)] = [0.02345, 0, 0.02021, 0]$, and take the aforementioned integration constants $c_1 = c_2 = 0.1$ and $c_3 = c_4 = 10000$. As shown in Figure 1, the solution (28) obtained by the two-timing scale method is almost the same as the solution of the original system (14) (so-called “exact solution”) at each time. Meantime, these two solutions display the same trend as time evolves. In summary, these reveal that the two-timing scale method effectively describes this complex nonlinear charged dilaton black hole system, and the obtained asymptotic solutions are resultful with some parameter values.

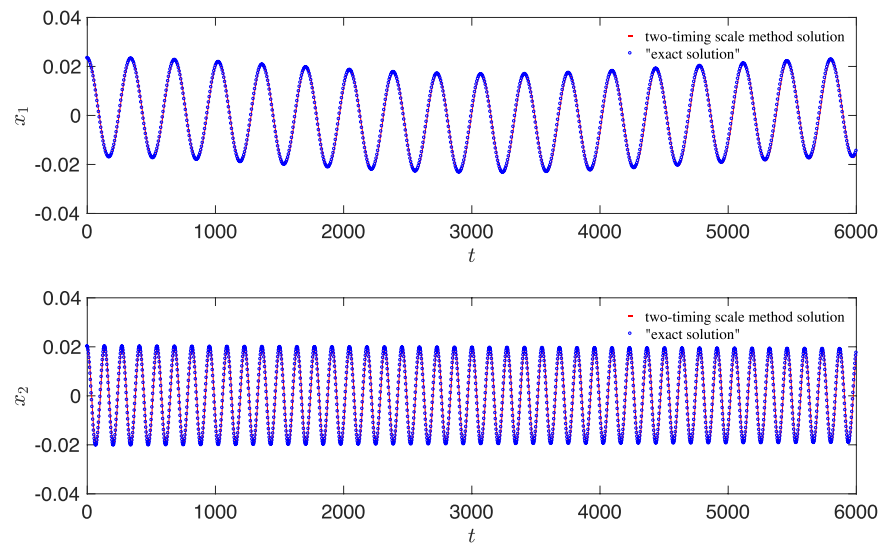


Figure 1. A comparison between the two-timing scale method solution and the “exact solution” for $q = 1, \alpha = 0.01, b = 1, A = 0.3703, s = 0.04, \mu_0 = 0.1, \omega = 0.01, \delta = 0.004$ and $\epsilon = 0.001$.

Moreover, at the same values of the above parameter, the phase portrait of the asymptotic solution is plotted as shown in Figure 2. Combining Figure 1 with Figure 2, it can be found that there exists a quasi-periodic motion, which is worthy of further study in the next section.

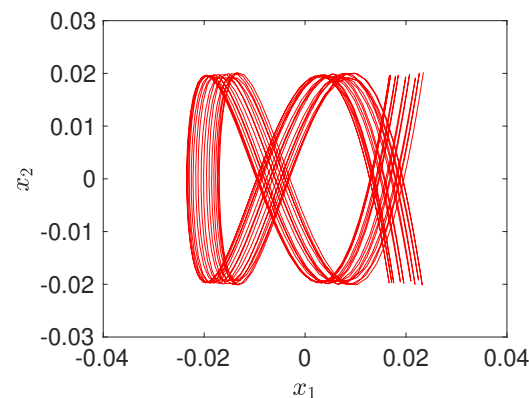


Figure 2. Phase portrait of the two-timing scale method solution.

In order to explore the final state of the black hole flow, the following equations are considered by neglecting the non-periodic terms in the Equation (28), which are denoted by the “asymptotic periodic solutions”

$$\begin{aligned}
 x_1 &= -\frac{\epsilon P_T \delta}{\omega^2 - \lambda_1^2} \cos \omega T_1 + \frac{\epsilon^2 \mu_0 s P_T \delta \omega}{(\lambda_1^2 - \omega^2)^2} \sin \omega T_1, \\
 x_2 &= -\frac{\epsilon^2 P_{vT} P_T \delta^2}{2(\omega^2 - \lambda_1^2)(\lambda_2^2 - 4\omega^2)} \cos 2\omega T_1 - \frac{\epsilon^2 P_{vT} P_T \delta^2}{4(\omega^2 - \lambda_1^2)\lambda_2^2}.
 \end{aligned}
 \tag{29}$$

Take $c_1 = c_2 = c_3 = c_4 = 10^{-6}$, a comparison between the asymptotic solution and asymptotic periodic solution is shown in Figure 3. It is clear that the non-periodic terms in Equation (28) have barely any effect on the obtained solutions when the order of magnitude of integration constants is small.

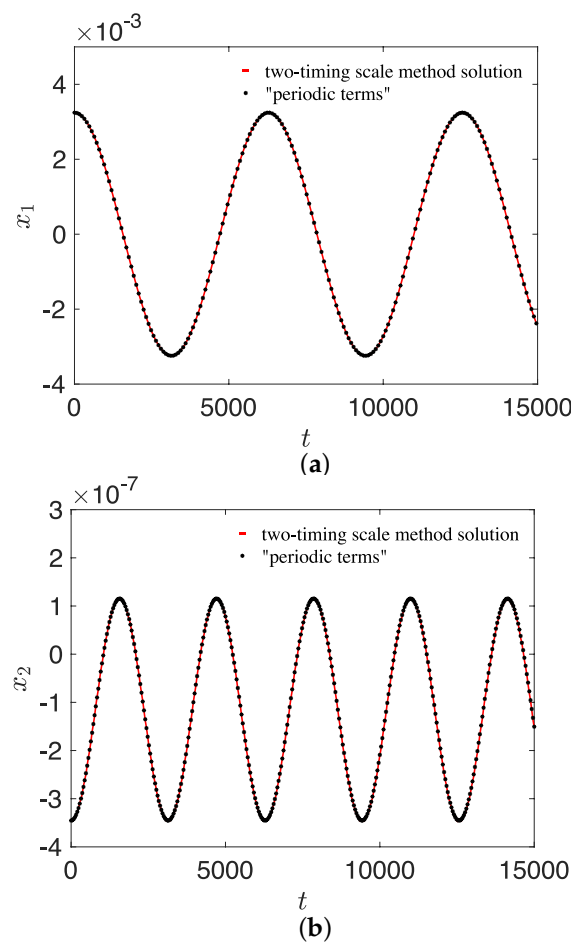


Figure 3. A comparison between the asymptotic solution and asymptotic periodic solution for $A = 0.3703, s = 0.04, \mu_0 = 0.1, \omega = 0.01, \delta = 0.004$ and $\epsilon = 0.001$: (a) Time-history diagram in x_1 -direction, (b) Time-history diagram in x_2 -direction.

5. Quasi-Periodic Behavior

Quasi-periodicity is a new type of long-term behavior, which is different from fixed point, homoclinic orbit, heteroclinic orbit, and periodic orbit. In deep space exploration, the Lissajous orbit and quasi-halo orbit near the Lagrangian points that have practical applications are also quasi-periodic. Mathematically, the frequencies in different directions are incommensurable, which implies that when the value of λ_1/λ_2 in Section 3 is an irrational number, the corresponding trajectory is said to be quasi-periodic. Then, as time evolves, the trajectory will never close into itself, which means that time-domain solutions will never be repeated. This is because any closed trajectory is bound to rotate an integer

circle about λ_1 and λ_2 , the frequency ratio must be a rational number. On the contrary, each trajectory will be dense as time flows.

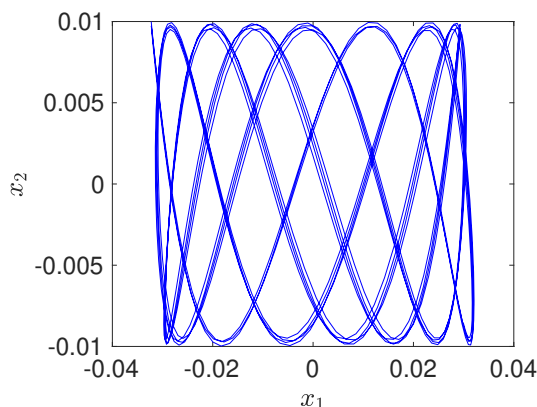
Based on the results in Section 4, it is worthy of studying the qualitative behavior of the “exact solution” of the charged dilaton black hole system (14). The quasi-periodic behavior characterized by the black hole flow is further studied in this section with different values of the parameters (see Table 1) and initial values of the black hole system. Note that the denominator of P_v contains the irrational number π ; then, it is obvious that there are constants T_0, v_0, q, α and b to make P_v an irrational number. Therefore,

$$\frac{\lambda_1}{\lambda_2} = \frac{\sqrt{As^2 - P_v}}{\sqrt{4As^2 - P_v}} = \sqrt{1 - \frac{3}{4 - \frac{P_v}{As^2}}}$$

is an irrational number for any rational constant $As^2 (> P_v)$. Then, several quasi-periodic motions are found and shown in Figures 4 and 5. For example, take $T_0 = 0.0315, v_0 = 3.652, \epsilon = 0.001, \mu_0 = 0.1, \omega = 0.01, \delta = 0.004, q = 1, \alpha = 0.01, b = 0.019836, A = 0.2$ and $s = 0.04$, and the initial value of the system as $[x_1(0), u_1(0), x_2(0), u_2(0)] = [-0.03226, 0, 0.01, 0]$. Then, the phase portrait shows a “reticular shape” in Figure 4a, which characterizes the quasi-periodic motion of the black hole flow. In addition, seven more quasi-periodic motions are shown below, which are similar to “V-shape”, “8-shape” and “pillow-shape” and so on.

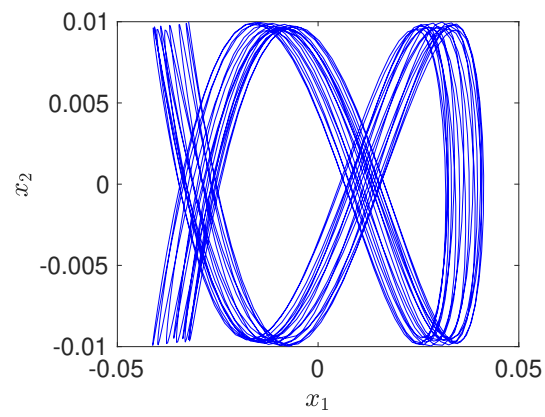
Table 1. Parameter values in the charged dilaton black hole flow.

Parameters	q	α	b	A	s
Group (a)	1	0.01	0.019836	0.2	0.04
Group (b)	1	0.01	1	0.3703	0.04
Group (c)	1	0.01	1	0.4884	0.04
Group (d)	1.0319	0.01	1	0.2	0.04
Group (e)	1	0.3	1	0.2	0.8
Group (f)	1	1.732	10,000	0.2	0.04

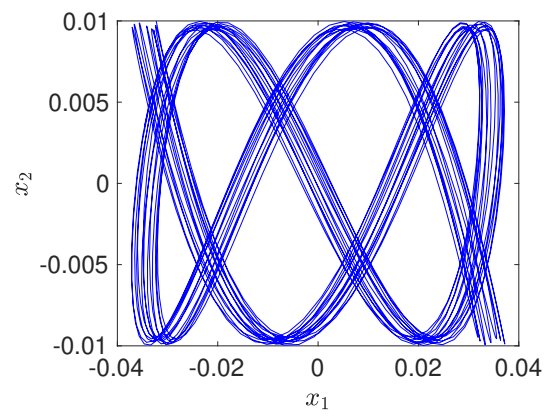


(a)

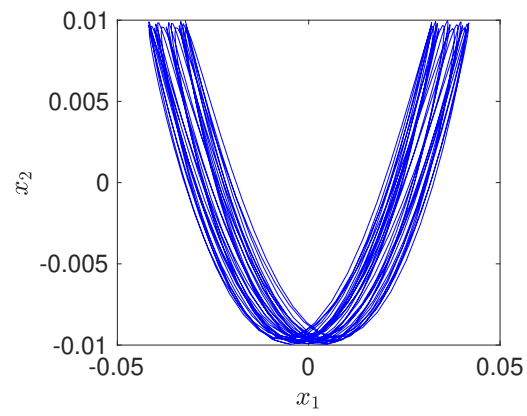
Figure 4. Cont.



(b)

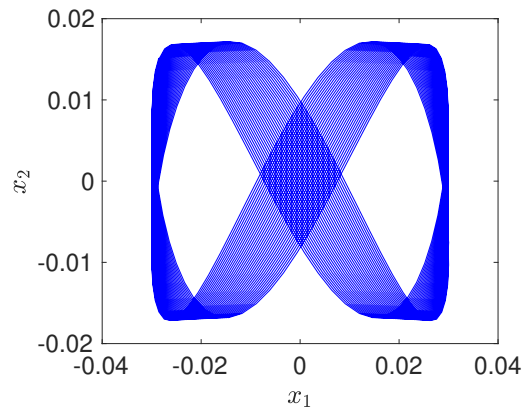


(c)

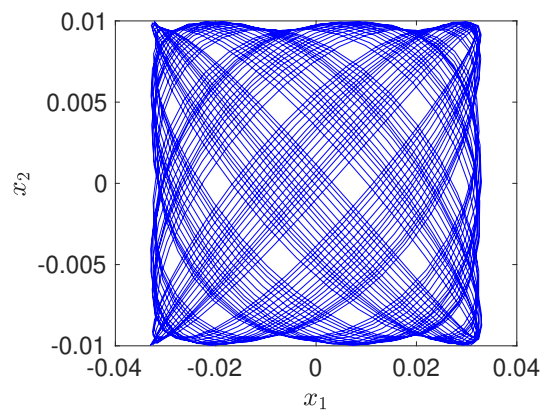


(d)

Figure 4. Cont.



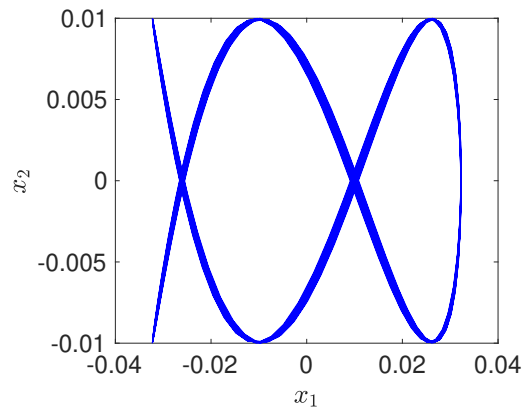
(e)



(f)

Figure 4. (a–f) Phase portraits of the charged dilaton black hole system corresponding to the six groups in Table 1 when $\epsilon = 0.001$.

Considering that the value of the thermal perturbation parameter ϵ is 0.000001, the related phase portraits of the system corresponding to the aforementioned Group (b) and Group (c) are shown in Figure 5. The phase trajectories of the system tend to be stable as time goes on. Moreover, the system’s motion tends to be periodic, and the vibration amplitude tends to be constant simultaneously.



(a)

Figure 5. Cont.

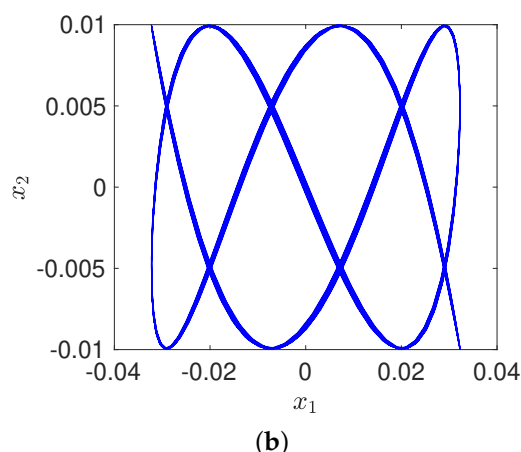


Figure 5. (a,b) Phase portraits of the charged dilaton black hole system for different λ_1/λ_2 with $\epsilon = 0.000001$.

6. Discussion and Conclusions

In this paper, the qualitative and quantitative analysis of charged dilation black holes is investigated. The two-timing scale method is applied to analyze the black hole flow equation and construct the second-order asymptotic analytical solution. According to these solutions, a numerical comparison with different system parameters values is carried out. By doing so, it can be found that these asymptotic solutions effectively describe the dynamical behavior of the black hole flow for a long time. At the same time, the relevant phase portraits are drawn to show quasi-periodic motion.

According to the obtained quasi-periodic motion, the quasi-periodic behavior of the black hole flow in the spinodal region is further studied when the frequency of λ_1/λ_2 is an irrational number. Several quasi-periodic motions with different parameter values are found. It is worth mentioning that when the thermal parameter perturbation takes a small value, the phase portraits of the black hole system exhibit better stability than the large value, and the vibration amplitude tends to be constant simultaneously.

Furthermore, to understand the final evolution state of the thermal dynamics of the black hole flow, the periodic solution is found according to the constructed analytical solution. The numerical comparison of these two solutions shows that they agree well for the small integral constant. In other words, the smaller the integral constant, the greater the extent of the black hole flow's motion tends to be periodic.

Author Contributions: Conceptualization, F.G.; Formal analysis, R.W.; software, R.W.; writing—original draft, R.W.; writing—review and editing, F.G. All authors have read and agreed to the published version of the manuscript.

Funding: This research was funded by the National Natural Science Foundation of China (NSFC) through grant nos. 12172322 and 11672259, the China Scholarship Council through grant No. 201908320086, the Postgraduate Research & Practice Innovation Program of Jiangsu Province (KYCX21_3190).

Institutional Review Board Statement: Not applicable.

Informed Consent Statement: Not applicable.

Data Availability Statement: Not applicable.

Acknowledgments: We are very grateful to the anonymous reviewers whose comments and suggestions helped improve and clarify this paper.

Conflicts of Interest: The authors declare no conflict of interest.

Appendix A

$$\begin{aligned}
 x_{11}^3 &= c_1^3 e^{-\frac{3\mu_0 s T_2}{2}} \left(e^{3i\lambda_1 T_1} + e^{-3i\lambda_1 T_1} + 3 e^{i\lambda_1 T_1} + 3 e^{-i\lambda_1 T_1} \right) \\
 &\quad - \frac{3c_1^2 P_T \delta e^{-\mu_0 s T_2}}{2(\omega^2 - \lambda_1^2)} \left[2 e^{i\omega T_1} + 2 e^{-i\omega T_1} + e^{i(2\lambda_1 + \omega) T_1} \right. \\
 &\quad \left. + e^{-i(2\lambda_1 + \omega) T_1} + e^{i(2\lambda_1 - \omega) T_1} + e^{i(\omega - 2\lambda_1) T_1} \right] \\
 &\quad + \frac{3c_1 P_T^2 \delta^2 e^{-\frac{\mu_0 s T_2}{2}}}{4(\omega^2 - \lambda_1^2)^2} \left[e^{i(\lambda_1 + 2\omega) T_1} + e^{-i(\lambda_1 + 2\omega) T_1} + e^{i(\lambda_1 - 2\omega) T_1} \right. \\
 &\quad \left. + e^{i(2\omega - \lambda_1) T_1} + 2 e^{i\lambda_1 T_1} + 2 e^{-i\lambda_1 T_1} \right] - \frac{P_T^3 \delta^3}{8(\omega^2 - \lambda_1^2)^3} \left(e^{3i\omega T_1} \right. \\
 &\quad \left. + e^{-3i\omega T_1} + 3 e^{i\omega T_1} + 3 e^{-i\omega T_1} \right), \\
 x_{11} x_{21}^2 &= c_1 c_2^2 e^{-\frac{9\mu_0 s T_2}{2}} \left[e^{i(\lambda_1 + 2\lambda_2) T_1} + e^{-i(\lambda_1 + 2\lambda_2) T_1} + e^{i(\lambda_1 - 2\lambda_2) T_1} \right. \\
 &\quad \left. + e^{i(2\lambda_2 - \lambda_1) T_1} + 2 e^{i\lambda_1 T_1} + 2 e^{-i\lambda_1 T_1} \right] - \frac{c_2^2 P_T \delta e^{-4\mu_0 s T_2}}{2(\omega^2 - \lambda_1^2)} \times \\
 &\quad \left[e^{i(\omega + 2\lambda_2) T_1} + e^{i(\omega - 2\lambda_2) T_1} + 2 e^{i\omega T_1} + 2 e^{-i\omega T_1} + e^{-i(\omega + 2\lambda_2) T_1} \right. \\
 &\quad \left. + e^{i(2\lambda_2 - \omega) T_1} \right], \\
 x_{11}^2 x_{21} &= c_1^2 c_2 e^{-3\mu_0 s T_2} \left[e^{i(2\lambda_1 + \lambda_2) T_1} + e^{i(2\lambda_1 - \lambda_2) T_1} + e^{i(\lambda_2 - 2\lambda_1) T_1} \right. \\
 &\quad \left. + e^{-i(2\lambda_1 + \lambda_2) T_1} \right] + 2 c_1^2 c_2 e^{-3\mu_0 s T_2} \left(e^{i\lambda_2 T_1} + e^{-i\lambda_2 T_1} \right) \\
 &\quad - \frac{c_1 c_2 P_T \delta e^{-\frac{5\mu_0 s T_2}{2}}}{\omega^2 - \lambda_1^2} \left[e^{i(\omega + \lambda_1 + \lambda_2) T_1} + e^{-i(\omega + \lambda_1 + \lambda_2) T_1} \right. \\
 &\quad \left. + e^{i(\omega + \lambda_1 - \lambda_2) T_1} + e^{i(\lambda_1 + \lambda_2 - \omega) T_1} + e^{i(\lambda_1 - \lambda_2 - \omega) T_1} \right. \\
 &\quad \left. + e^{i(\omega - \lambda_1 + \lambda_2) T_1} + e^{i(\omega - \lambda_1 - \lambda_2) T_1} + e^{i(\lambda_2 - \omega - \lambda_1) T_1} \right] \\
 &\quad + \frac{c_2 P_T^2 \delta^2 e^{-2\mu_0 s T_2}}{4(\omega^2 - \lambda_1^2)^2} \left[2 e^{i\lambda_2 T_1} + 2 e^{-i\lambda_2 T_1} + e^{i(\lambda_2 + 2\omega) T_1} \right. \\
 &\quad \left. + e^{-i(\lambda_2 + 2\omega) T_1} + e^{i(\lambda_2 - 2\omega) T_1} + e^{i(2\omega - \lambda_2) T_1} \right].
 \end{aligned}$$

References

1. Oppenheimer, J.R.; Snyder, H. On continued gravitational contraction. *Phys. Rev.* **1939**, *56*, 455–459. [\[CrossRef\]](#)
2. Webster, B.L.; Murdin, P. Cygnus X-1-a spectroscopic binary with a heavy companion? *Nature* **1972**, *235*, 37–38. [\[CrossRef\]](#)
3. Campanelli, M.; Lousto, C.; Zlochower, Y.; Merritt, D. Large merger recoils and spin flips from generic black-hole binaries. *Astrophys. J.* **2007**, *659*, L5–L8. [\[CrossRef\]](#)
4. Podsiadlowski, P.; Rappaport, S.; Han, Z. On the formation and evolution of black hole binaries. *Mon. Not. R. Astron. Soc.* **2010**, *341*, 385–404. [\[CrossRef\]](#)
5. Abbott, B.P.; Abbott, R.; Abbott, T.D.; Abernathy, M.R.; Acernese, F.; Ackley, K.; Adams, C.; Adams, T.; Addesso, P.; Adhikari, R.X.; et al. Observation of gravitational waves from a binary black hole merger. *Phys. Rev. Lett.* **2016**, *116*, 061102. [\[CrossRef\]](#)
6. Abbott, B.P.; Abbott, R.; Abbott, T.D.; Abernathy, M.R.; Acernese, F.; Ackley, K.; Adams, C.; Adams, T.; Addesso, P.; Adhikari, R.X.; et al. GW151226: Observation of gravitational waves from a 22-solar-mass binary black hole coalescence. *Phys. Rev. Lett.* **2016**, *116*, 241103. [\[CrossRef\]](#)
7. Abbott, R.; Abbott, T.D.; Abraham, S.; Acernese, F.; Ackley, K.; Adams, A.; Adams, C.; Adhikari, R.X.; Adya, V.B.; Affeldt, C.; et al. Observation of gravitational waves from two neutron star-black hole coalescences. *Astrophys. J. Lett.* **2021**, *915*, L5. [\[CrossRef\]](#)
8. Alexeyev, S.; Sendyuk, M. Black holes and wormholes in extended gravity. *Universe* **2020**, *6*, 25. [\[CrossRef\]](#)

9. Stuchlík, Z.; Vrba, J. Epicyclic oscillations around Simpson-Visser regular black holes and wormholes. *Universe* **2021**, *7*, 279. [[CrossRef](#)]
10. Kiritsis, E.; Kofinas, G. On Hořava-Lifshitz “black holes”. *J. High Energy Phys.* **2010**, *2010*, 122. [[CrossRef](#)]
11. Poshteh, M.B.J.; Riazi, N. Phase transition and thermodynamic stability in extended phase space and charged Hořava-Lifshitz black holes. *Gen. Relativ. Gravit.* **2017**, *49*, 64. [[CrossRef](#)]
12. Gao, F.B.; Llibre, J. Global dynamics of Hořava-Lifshitz cosmology with non-zero curvature and a wide range of potentials. *Eur. Phys. J.* **2020**, *80*, 137. [[CrossRef](#)]
13. Król, J.; Klimasara, P. Black holes and complexity via constructible universe. *Universe* **2020**, *6*, 198. [[CrossRef](#)]
14. Marto, J. Hawking radiation and black hole gravitational back reaction—A quantum geometrodynamical simplified model. *Universe* **2021**, *7*, 297. [[CrossRef](#)]
15. Hawking, S.W. Black hole explosions? *Nature* **1974**, *248*, 30–31. [[CrossRef](#)]
16. Hawking, S.W. Black holes and thermodynamics. *Phys. Rev. D* **1976**, *13*, 55–97. [[CrossRef](#)]
17. Hawking, S.W.; Page, D.N. Thermodynamics of black holes in anti-de Sitter space. *Commun. Math. Phys.* **1983**, *87*, 577–588. [[CrossRef](#)]
18. Wald, R.M. The thermodynamics of black holes. *Living Rev. Relativ.* **2001**, *4*, 6. [[CrossRef](#)]
19. Hayward, S.A. Unified first law of black-hole dynamics and relativistic thermodynamics. *Class. Quantum Gravity* **1998**, *15*, 3147–3162. [[CrossRef](#)]
20. Hendi, S.H.; Sajadi, S.N.; Khademi, M. Physical properties of a regular rotating black hole: Thermodynamics, stability, and quasinormal modes. *Phys. Rev. D* **2021**, *103*, 064016. [[CrossRef](#)]
21. Gallerati, A. New black hole solutions in $N = 2$ and $N = 8$ gauged supergravity. *Universe* **2021**, *7*, 187. [[CrossRef](#)]
22. Xiao, Y.; Chen, Y.; Feng, H.Y.; Zhu, C.R. Black hole solutions and thermodynamics in the infinite derivative theory of gravity. *Phys. Rev. D* **2021**, *103*, 044064. [[CrossRef](#)]
23. Chamblin, A.; Emparan, R.; Johnson, C.V.; Myers, R.C. Holography, thermodynamics, and fluctuations of charged AdS black holes. *Phys. Rev. D* **1999**, *60*, 104026. [[CrossRef](#)]
24. Wu, X.N. Multicritical phenomena of Reissner-Nordström anti-de Sitter black holes. *Phys. Rev. D* **2000**, *62*, 124023. [[CrossRef](#)]
25. Dehghani, M.H.; Kamrani, S.; Sheykhi, A. P - V criticality of charged dilatonic black holes. *Phys. Rev. D* **2014**, *90*, 104020. [[CrossRef](#)]
26. Zhang, M.; Yang, Z.Y.; Zou, D.C.; Xu, W.; Yue, R.H. P - V criticality of AdS black hole in the Einstein-Maxwell-power-Yang-Mills gravity. *Gen. Relativ. Gravit.* **2014**, *47*, 14. [[CrossRef](#)]
27. Hu, Y.P.; Zeng, H.A.; Jiang, Z.M.; Zhang, H. P - V criticality in the extended phase space of black holes in Einstein-Horndeski gravity. *Phys. Rev. D* **2019**, *100*, 084004. [[CrossRef](#)]
28. Hendi, S.H.; Dehghani, A. Criticality and extended phase space thermodynamics of AdS black holes in higher curvature massive gravity. *Eur. Phys. J. C* **2019**, *79*, 227. [[CrossRef](#)]
29. Sharif, M.; Ama-Tul-Mughani, Q. P - V criticality and phase transition of the Kerr-Sen-AdS black hole. *Eur. Phys. J. Plus* **2021**, *136*, 284. [[CrossRef](#)]
30. Liang, J. The P - v criticality of a noncommutative geometry-inspired Schwarzschild-AdS black hole. *Chin. Phys. Lett.* **2017**, *34*, 080402. [[CrossRef](#)]
31. Chen, S.B.; Liu, X.F.; Liu, C.Q. P - V criticality of an AdS black hole in $f(R)$ gravity. *Chin. Phys. Lett.* **2013**, *30*, 060401. [[CrossRef](#)]
32. Liang, J.; Guan, Z.H.; Liu, Y.C.; Liu, B. P - v criticality in the extended phase space of a noncommutative geometry inspired Reissner-Nordström black hole in AdS space-time. *Gen. Relativ. Gravit.* **2017**, *49*, 29. [[CrossRef](#)]
33. Li, R.; Wang, J. Hawking radiation and P - v criticality of charged dynamical (Vaidya) black hole in anti-de Sitter space. *Phys. Lett. B* **2021**, *813*, 136035. [[CrossRef](#)]
34. Zhao, H.H.; Zhang, L.C.; Zhao, R. Two-phase equilibrium properties in charged topological dilaton AdS black holes. *Adv. High Energy Phys.* **2016**, *2016*, 2021748. [[CrossRef](#)]
35. Sherkatghanad, Z.; Mirza, B.; Mirzaiyan, Z.; Mansoori, S.A.H. Critical behaviors and phase transitions of black holes in higher order gravities and extended phase spaces. *Int. J. Mod. Phys. D* **2017**, *26*, 1750017. [[CrossRef](#)]
36. Hendi, S.H.; Nemati, A.; Lin, K.; Jamil, M. Instability and phase transitions of a rotating black hole in the presence of perfect fluid dark matter. *Eur. Phys. J. C* **2020**, *80*, 296. [[CrossRef](#)]
37. Dehyadegari, A.; Sheykhi, A.; Montakhab, A. Novel phase transition in charged dilaton black holes. *Phys. Rev. D* **2017**, *96*, 084012. [[CrossRef](#)]
38. Liang, K.; Wang, P.; Wu, H.; Yang, M. Phase structures and transitions of Born-Infeld black holes in a grand canonical ensemble. *Eur. Phys. J. C* **2020**, *80*, 187. [[CrossRef](#)]
39. Ma, Y.; Zhang, Y.; Zhang, L.; Wu, L.; Gao, Y.; Cao, S.; Pan, Y. Phase transition and entropic force of de Sitter black hole in massive gravity. *Eur. Phys. J. C* **2021**, *81*, 42. [[CrossRef](#)]
40. Chabab, M.; El Mounni, H.; Iraoui, S.; Masmar, K. Phase transitions and geothermodynamics of black holes in dRGT massive gravity. *Eur. Phys. J. C* **2019**, *79*, 342. [[CrossRef](#)]
41. Hendi, S.H.; Azari, F.; Rahimi, E.; Elahi, M.; Owjifard, Z.; Armanfard, Z. Thermodynamics and the phase transition of topological dilatonic Lifshitz-like black holes. *Ann. Der Phys.* **2020**, *532*, 2000162. [[CrossRef](#)]
42. Wang, P.; Wu, H.W.; Yang, H.T. Thermodynamics and phase transition of a nonlinear electrodynamic black hole in a cavity. *J. High Energy Phys.* **2019**, *2019*, 002. [[CrossRef](#)]

43. Wang, P.; Wu, H.W.; Yang, H.T. Thermodynamics and phase transitions of nonlinear electrodynamics black holes in an extended phase space. *J. Cosmol. Astropart. Phys.* **2019**, *2019*, 052. [[CrossRef](#)]
44. Zhang, L.C.; Ma, M.S.; Zhao, H.H.; Zhao, R. Thermodynamics of phase transition in higher-dimensional Reissner-Nordström-de Sitter black hole. *Eur. Phys. J. C* **2014**, *74*, 3052. [[CrossRef](#)]
45. Qiu, J.H.; Gao, C.J. Constructing higher-dimensional exact black holes in Einstein-Maxwell-scalar theory. *Universe* **2020**, *6*, 148. [[CrossRef](#)]
46. Guo, X.Y.; Li, H.F.; Zhang, L.C.; Zhao, R. Continuous phase transition and microstructure of charged AdS black hole with quintessence. *Eur. Phys. J. C* **2020**, *80*, 168. [[CrossRef](#)]
47. Chen, Y.; Li, H.T.; Zhang, S.J. Chaos in Born-Infeld-AdS black hole within extended phase space. *Gen. Relativ. Gravit.* **2019**, *51*, 134. [[CrossRef](#)]
48. Dai, C.Q.; Chen, S.B.; Jing, J.L. Thermal chaos of a charged dilaton-AdS black hole in the extended phase space. *Eur. Phys. J. C* **2020**, *80*, 245. [[CrossRef](#)]
49. Chabab, M.; El Moumni, H.; Iraoui, S.; Masmar, K.; Zhizeh, S. Chaos in charged AdS black hole extended phase space. *Phys. Lett. B* **2018**, *78*, 316–321. [[CrossRef](#)]
50. Mahish, S.; Bhamidipati, C. Chaos in charged Gauss-Bonnet AdS black holes in extended phase space. *Phys. Rev. D* **2019**, *99*, 106012. [[CrossRef](#)]
51. Tang, B. Temporal and spatial chaos in the Kerr-AdS black hole in an extended phase space. *Chin. Phys. C* **2021**, *45*, 055101. [[CrossRef](#)]
52. Guo, X.; Liang, K.; Mu, B.; Wang, P.; Yang, M. Chaotic motion around a black hole under minimal length effects. *Eur. Phys. J. C* **2020**, *80*, 745. [[CrossRef](#)]
53. Zhou, X.; Chen, S.B.; Jing, J.L. Chaotic motion of scalar particle coupling to Chern-Simons invariant in Kerr black hole spacetime. *Eur. Phys. J. C* **2021**, *81*, 233. [[CrossRef](#)]
54. Shafiq, S.; Hussain, S.; Ozair, M.; Aslam, A.; Hussain, T. Charged particle dynamics in the surrounding of Schwarzschild anti-de Sitter black hole with topological defect immersed in an external magnetic field. *Eur. Phys. J. C* **2020**, *80*, 744. [[CrossRef](#)]
55. Hussain, S.; Hussain, I.; Jamil, M. Dynamics of a charged particle around a slowly rotating Kerr black hole immersed in magnetic field. *Eur. Phys. J. C* **2014**, *74*, 3210. [[CrossRef](#)]
56. Strogatz, S.H. *Nonlinear Dynamics and Chaos*; CRC Press, Taylor & Francis Group: Boca Raton, FL, USA, 2018.
57. Sheykhi, A. Thermodynamics of charged topological dilaton black holes. *Phys. Rev. D* **2007**, *76*, 124025. [[CrossRef](#)]
58. Sheykhi, A. Topological Born-Infeld-dilaton black holes. *Phys. Lett. B* **2008**, *662*, 7–13. [[CrossRef](#)]
59. Slemrod, M.; Marsden, J.E. Temporal and spatial chaos in a van der Waals fluid due to periodic thermal fluctuations. *Adv. Appl. Math.* **1985**, *6*, 135–158. [[CrossRef](#)]
60. Melnikov, V.K. On the stability of the center for time periodic perturbations. *Trans. Mosc. Math. Soc.* **1963**, *12*, 3–52.